

SCIENCE & TECHNOLOGY

Journal homepage: http://www.pertanika.upm.edu.my/

A Single-stage LED Driver with Voltage Doubler Rectifier

Nurul Asikin, Zawawi^{1*}, Shahid Iqbal¹ and Mohamad Kamarol, Mohd Jamil¹

School of Electrical and Electronic Engineering, Universiti Sains Malaysia, Nibong Tebal, 14300 Penang, Malaysia

ABSTRACT

In this paper, a configuration of a single-stage AC-DC converter and a high voltage resonant controller IC L6598 for LED street light driver is discussed. The converter is obtained by integrating two boost circuits and a half-bridge LLC resonant circuit. A voltage double rectifier circuit is adopted as output to lower the voltage stress on transformer and the associated core. The two boost circuits work in boundary conduction mode (BCM) to achieve the power factor correction (PFC). The converter works in soft-switching mode allowing the power switches to operate in zero-voltage-switching (ZVS) and the output diodes to operate in zero-current-switching (ZCS). This reduces the switching losses and enhances the efficiency. The converter features lower voltage stress on the power switches and the bus voltage is reduced to slightly higher than the peak input voltage. Therefore, the converter can perform well under high-input-voltage. Here, the DC bus and the output filter capacitances are greatly reduced. So, electrolytic capacitor-less converter can be realized for a long lifetime LED driver. Simulation results from PSpice are presented for a 100-W prototype.

Keywords: LED driver, boost circuit, LLC, power factor correction, street lighting, voltage doubler

INTRODUCTION

Recently, light-emitting diode (LED) has become popular for street lighting due to its energy savings capacity and low maintenance

ARTICLE INFO

Article history:

Received: 24 August 2016 Accepted: 02 December 2016

E-mail addresses: nurulasikinz@hotmail.com (Nurul Asikin, Zawawi), shahisidu@hotmail.com (Shahid Iqbal), eekamarol@usm.my (Mohamad Kamarol, Mohd Jamil) *Corresponding Author

costs. Switching from incandescent lights to LEDs can also help reduce greenhouse gas emissions from power plants in addition to providing better light quality and eliminating mercury waste disposal ("Energy Efficient," 2013).

An appropriate converter that can support a wide range of universal input ac voltages is desirable. Therefore, AC-DC conversion stage is a compulsory to drive the system powered from ac source. Switching converter is usually chosen due to its economical driving solutions, but the conventional AC-

ISSN: 0128-7680 © 2017 Universiti Putra Malaysia Press.

DC switching converters have poor performances in PF and harmonic distortion. In order to achieve input current shaping, an additional PFC stage is added in front of the converters. In spite of its good performance, these two-stage converters are usually expensive, bigger in size and energy inefficient compared to the single-stage converters. To simplify the circuit and improve the reliability of the system, single-stage AC-DC converters were proposed (Gacio et al., 2011; Lin et al., 2006; Lu et al., 2008). PFC circuit and the DC-DC converter were integrated into one stage by sharing one or more switches. However, the integrated switch was subjected to high voltage stress and operated in hard switching which decreases the circuit efficiency.

A single-stage LLC resonant converter has the advantage of soft-switching characteristics and can achieve high efficiency. However, the single-stage PFC converters based on half-bridge resonant structure (Chen et al., 2012; Kang et al., 2002; Lai & Shyu, 2007) continued to maintain a high bus voltage twice the input peak voltage. On the contrary, the converter in Seok & Kwon, 2001 demonstrated a lower bus voltage, and less voltage stress on the switching devices. Wang et al. (2010) proposed a single-stage LED driver which comprises an interleaving boost circuit and half-bridge LLC resonant circuit. The two boost circuits work in DCM to obtain PFC function. With proper switching frequency, the primary-side switches operate in ZVS and the secondary-side diodes operate in ZCS. Cheng and Yen (2011) implemented the same topology and reduced one capacitor at the input side. Later, Wang et al. (2015) improved the topology by replacing the two boost inductors with a single inductor that was shared by the two boost circuits. Both boost circuits worked in BCM. However, the driver is more complex and larger in terms of its size since it uses pulse transformer for the driving circuit.

In this paper, the configuration of a single-stage LED driver proposed in Wang et al., 2015 and a resonant controller ICL658 is used to design a 100-W prototype for application under 240-V AC input. Since the voltage divider capacitors can fulfil the same role, the driver eliminated the DC input filter capacitor after the input bridge rectifier. By employing the output-voltage doubler rectifier on the secondary side, a higher voltage conversion ratio is obtained with a lower turn ratio transformer. The reduced turn ratio increases the overall efficiency. The transformer size also can be decreased. Here, the output voltage is shared by two output filter capacitors. So, a smaller capacitance with lower voltage rating capacitor can be used. Since, the DC bus and the output filter capacitance are incredibly downsized; film type capacitor can be utilized. Hence, a longer life span for the LED driver can be achieved.

Structure of the proposed circuit

Figure 1 shows the proposed configuration of LED driver with a resonant controller and a control circuit. The driver consists of a full-bridge rectifier, two voltage divider capacitors C_I and C_2 , two boost diodes D_I and D_2 , a boost inductor L_b , two power switches S_I and S_2 , a bus voltage capacitor C_{bus} , a resonant capacitor C_r , a transformer with resonant inductor L_r and magnetizing inductor L_m , two output diodes D_{rI} and D_{r2} , two output capacitors C_{rI} and C_{r2} and LED street light module. Here, C_{SI} and C_{S2} are the parasitic capacitors, while D_{SI} and D_{S2} are the parasitic diodes of switches S_I and S_I . Two boost circuits are obtained by integrating the switches of half-bridge LLC resonant circuit. C_{bus} , D_I , L_b , S_I , and D_{S2} constitute one boost circuit, whereas C_{bus} , D_2 , C_2 , C_3 , and C_3 constitute another boost circuit. C_{bus} and C_3 are shared by the two boost

circuits. A high voltage resonant controller IC manufactured by ST Microelectronics, L6598 would be used to drive the two switches alternately with a certain dead time and switching duty cycle nearly 0.5. The dead time provided between the conduction of the high-side switch and low-side switch will allows the switches to turn on with ZVS. The auxiliary voltage *Vaux* supply a constant voltage to the resonant controller for driving the switches.

Principle of the operation

This driver has ten operational modes in a single switching period. The steady state operating waveforms of the driver are demonstrated in Figure 2. In the following, the descriptions for the operational modes are elaborated.

Mode 1 $(t_0 - t_I)$: At time t_0 , switch S_2 is already turned off. Resonant current i_r flows in opposite direction through switch S_I to discharges parasitic capacitor C_{SI} . Hence, drain-source voltage V_{DSI} decreases to zero and parasitic diode D_{SI} is turned on. During this time, boost inductor L_b discharges energy via D_{SI} , C_{bus} , D_2 , and C_2 . On the secondary side, diode D_{rI} is turned on and current i_{DrI} increases. So, the voltage across magnetizing inductor L_m is clamped by output voltage. Resonant inductor L_r and resonant capacitor C_r form a resonant tank. Afterward, gate signal V_{GSI} arrives to turn on S_I in ZVS. At the end of this mode, i_r becomes zero.

Mode 2 $(t_1 - t_2)$: Within this time interval, resonant current i_r flows in positive direction and increases with sinusoidal shape.

Mode 3 $(t_2 - t_3)$: At time t_2 , parasitic diode D_{SI} is turned off. Resonant current i_r flows through C_{bus} and S_I . Magnetizing current i_m continues to decrease linearly. At the end of this mode, boost inductor L_b is completely discharged until current i_{Lb} becomes zero.

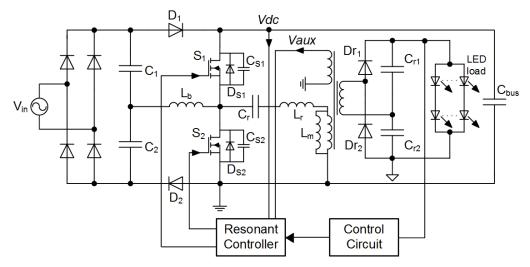


Figure 1. The proposed configuration of LED driver with a resonant controller and a control circuit

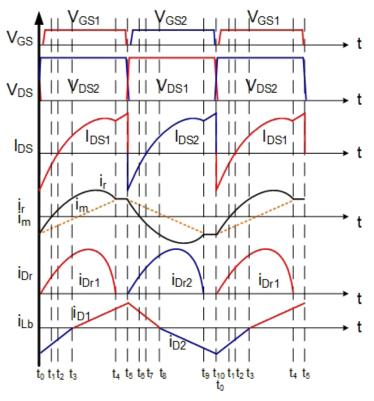


Figure 2. The steady state operating waveforms of the driver

Mode 4 $(t_3 - t_4)$: At time t_3 , C_1 charges L_b via D_1 and S_1 . Magnetizing current i_m becomes zero, then changes its flow to positive direction and continues to increase linearly to the maximum value. Resonant current i_r also increases until reaching the peak value then decreases until the value is equal to i_m . The difference current between i_r and i_m flows through the primary winding of the transformer and power is supplied to the load. Here, diode current i_{Dr1} increases to the peak value and then decreases to zero.

Mode 5 $(t_4 - t_5)$: At time t_4 , diode D_{rl} is turned off in ZCS. The secondary side circuit is separated from the primary side circuit. So, the voltage across L_m is no longer clamped by output voltage. Hence, L_m involves in the resonant tank with L_r and C_r . At this time, i_r and i_m are equal. The current continues to flow through C_{bus} and S_l . At the end of this mode, switch S_l is turned off. Parasitic capacitor C_{Sl} is charged and drain-source voltage V_{DSl} increases to bus voltage. Boost inductor L_b is fully charged and i_{Lb} reaches peak value.

Mode 6 $(t_5 - t_6)$: At time t_5 , resonant current i_r flows through switch S_2 and discharges parasitic capacitor C_{S2} . Hence, drain-source voltage V_{DS2} decreases to zero and parasitic diode D_{S2} is turned on. During this time, boost inductor L_b discharges energy via C_1 , D_1 , C_{bus} , and D_{S2} . On the secondary side, diode D_{r2} is turned on and current i_{Dr2} increases. So, the voltage across L_m is clamped by output voltage. Resonant inductor L_r and resonant capacitor C_r form a resonant tank. Afterward, gate signal V_{GS2} arrives to turn on S_2 in ZVS. At the end of this mode, i_r decreases to zero.

Mode 7 ($t_6 - t_7$): During this mode, resonant current i_r flows in negative direction and increases with sinusoidal shape.

Mode 8 ($t_7 - t_8$): At time t_7 , parasitic diode D_{S2} is turned off. Resonant current i_r flows through S_2 . Magnetizing current i_m continues to decrease linearly. At the end of this mode, boost inductor L_b is completely discharged until current i_{Lb} becomes zero.

Mode 9 ($t_8 - t_9$): At time t_8 , C_2 charges L_b via S_2 and D_2 . Magnetizing current i_m becomes zero, then changes its flow to negative direction and continues to increase linearly to the maximum value. Resonant current i_r also increases until reaching the peak value then decreases until the value is equal to i_m . The difference current between i_r and i_m flows through the primary winding of the transformer and power is supplied to the load. Here, diode current i_{Dr2} increases to the peak value and then decreases to zero.

Mode 10 $(t_9 - t_{I0})$: At time t_9 , diode D_{r2} is turned off in ZCS. The secondary side circuit is separated from the primary side circuit. So, the voltage of L_m is no longer clamped by output voltage. Hence, L_m involves in the resonant tank with L_r and C_r . At this time, i_r and i_m is equal. The current continues to flow through switch S_2 . At the end of this mode, switch S_2 is turned off. Parasitic capacitor C_{S2} is charged and drain-source voltage V_{DS2} increases to bus voltage. Boost inductor L_b is fully charged and i_{Lb} reaches peak value.

From the waveforms, the boost inductor current i_{Lb} is naturally in BCM state. The two boost circuits charge and discharge the energy to boost inductor L_b alternately in one switching period.

The switch is turned on when the drain-source voltage is zero. During this time, the parasitic diode carries reverse current before the switch conducts forward current. Hence, there are no turn on switching losses exist in the switches. Furthermore, when the switch is turned off, the parasitic capacitor will be charged and the drain-source voltage increases. At the same time, the parasitic capacitor of the opposite switch will be discharged and the energy stored is returned to the dc source. Here, capacitive loss is eliminated. This help to erase the turn off switching losses. Thus, the switches operate alternately with ZVS.

On the secondary side, output diodes are turned off with ZCS. Then, the secondary side is separated from the primary side and the output filter capacitors will supply energy to the LEDs.

Design consideration

A prototype of an LED driver is designed for application under 240-V AC input. Here, the LED street light module consists of six strings with two LEDs per sring. The LED has steady state rated performance of 26.5V/320mA. The switching frequency f_s of LLC resonant circuit must satisfy the range $f_m < f_s < f_r$ for the switches to work in ZVS and the secondary side diodes to work in ZCS. Here, the switching frequency is set to $0.9 f_r$. A large value of L_m is used to obtain a lower bus voltage in variation of the load. The utilized components for the driver are shown in detail in Table 1.

Table 1

Component list

Component	Symbol	Value
Voltage Divider Capacitor	C_1 , C_2	330nF
Boost Inductor	L_b	200uH
Resonant Capacitor	C_r	10nF
Leakage Inductor	L_r	110uH
Magnetizing Inductor	L_m	990uH
Bus Capacitor	C_{bus}	90uF
Output Capacitor	C_{rl} , C_{r2}	47uF

Simulation result

In this paper, a 100-W prototype with 53V output for an LED street light module is simulated using PSpice. Figure 3 shows the waveforms of the input voltage v_{in} and input current i_{in} . The input current is in phase with the input voltage, so the PFC function is obtained. The sinusoidal waveform without shape distortion portray that the current consist of fundamental component, so a low current THD can be estimated.

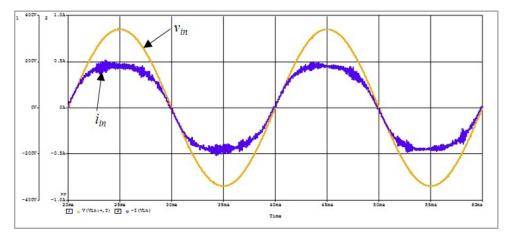


Figure 3. The waveforms of the input voltage v_{in} and input current i_{in}

Figure 4 shows the waveforms of V_{DSI} , V_{GSI} and I_{DSI} . The switch gate voltage V_{GSI} comes after the switch drain-source voltage V_{DSI} turned to zero. During this time, the switch conducts reverse current. This is demonstrating that the switches work in ZVS mode. Figure 5 shows the waveforms of the switch drain-source voltage V_{DSI} and diode current i_{DrI} . The diode current slowly decreases to zero and there is a short time it to keep it at zero value, which shows that the secondary side diodes turn off in ZCS mode.

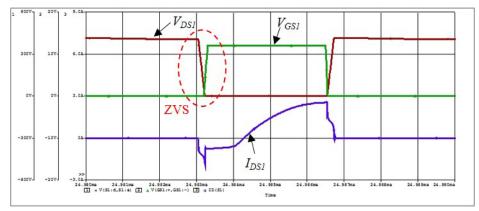


Figure 4. The waveforms of the switch drain-source voltage V_{DSI} , switch gate voltage V_{GSI} and switch current I_{DSI}

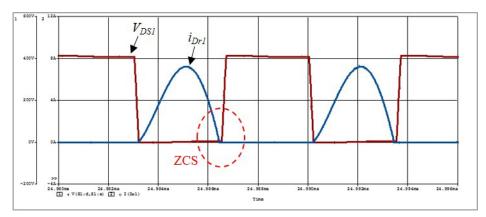


Figure 5. The waveforms of the switch drain-source voltage V_{DSI} and output diode current i_{DrI}

Figure 6 shows the waveforms of V_{DSI} , i_r , i_{DrI} and i_{Lb} in 100-W full-load stage. The resonant current i_r has a step shape and the diode current i_{DrI} works in ZCS. The switching frequency is 141 kHz.

Figure 7 shows the waveforms of output voltage V_o and output current I_o . The voltage is 53 V, and the current is 1.9 A, hence, the output power is approximately 100 W. The voltage ripple is lower than 1 V, while the current ripple is lower than 100 mA, which is an acceptable value to drive the LEDs without flicker.

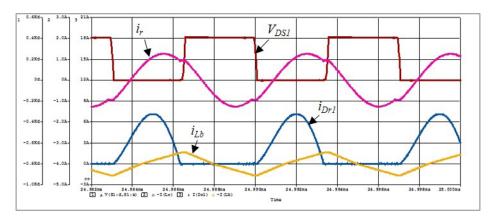


Figure 6. The waveforms of the switch drain-source voltage V_{DSI} , resonant current i_r , output diode current i_{DrI} and boost inductor current i_{Lb}

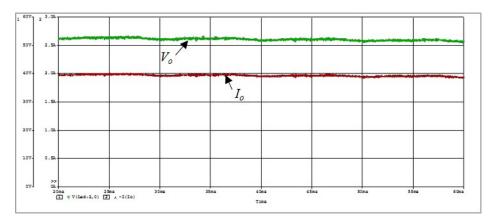


Figure 7. The waveforms of the output voltage V_o and output current I_o

CONCLUSION

A 100-W single-stage LED driver based on two boost circuits and a half-bridge type LLC resonant circuit is simulated under 240-V AC input. The boost circuits share a single inductor that operate in BCM to obtain the PFC. Input voltage is divided by two capacitors, so the voltage stress of the switches is reduced by half and the driver is suitable for high-input-voltage condition. The value of the magnetizing inductor is selected to be high so that the bus voltage is low in variation of the power. Both switches work with soft-switching characteristics in order to achieve a high conversion efficiency. Simulation results showed that the bus voltage was about 400V, which is higher than the input peak voltage. Here, ideal elements were selected, thus, the switches or components losses were not considered throughout the simulation.

ACKNOWLEDGEMENT

The authors would like to thank the Universiti Sains Malaysia for providing all necessary facilities and equipment to make this research possible. This work was supported by Fundamental Research Grant Scheme (FRGS) 203/PELECT/6071307 from Ministry of Education Malaysia.

REFERENCES

- Chen, S. Y., Li, Z. R., & Chen, C. L. (2012). Analysis and design of single-stage AC/DC LLC resonant converter. *IEEE Transactions on Industrial Electronics*, 59(3), 1538-1544.
- Cheng, C. A., & Yen, C. H. (2011, June 21-23). A single-stage driver for high power LEDs. Paper presented at the IEEE Conference on Industrial Electronics and Applications (pp. 2666-2671).
- Gacio, D., Alonso, J. M., Calleja, A. J., Garcia, J., & Rico-Secades, M. (2011). A universal-input single-stage high-power-factor power supply for HB-LEDs based on integrated buck–flyback converter. IEEE Transactions on Industrial Electronics, 58(2), 589-599.
- Kang, F. S., Park, S. J., & Kim, C. U. (2002). ZVZCS single-stage PFC AC-to-DC half-bridge converter. IEEE Transactions on Industrial Electronics, 49(1), 206-216.
- Lai, C. M., & Shyu, K. K. (2007). A single-stage AC/DC converter based on zero voltage switching LLC resonant topology. *IET Electric Power Applications*, 1(5), 743-752.
- Lau, S. P., Merrett, G. V., & White, N. M. (2013, May). Energy-efficient street lighting through embedded adaptive intelligence. In *Advanced Logistics and Transport (ICALT)*, 2013 International Conference on (pp. 53-58). IEEE.
- Lin, J. L., Yao, W. K., & Yang, S. P. (2006). Analysis and design for a novel single-stage high power factor correction diagonal half-bridge forward AC-DC converter. *IEEE Transactions on Circuits and Systems I: Regular Papers*, 53(10), 2274-2286.
- Lu, D. D. C., Iu, H. H. C., & Pjevalica, V. (2008). A single-stage AC/DC converter with high power factor, regulated bus voltage, and output voltage. *IEEE Transactions on Power Electronics*, 23(1), 218-228.
- Seok, K. W., & Kwon, B. H. (2001). A novel single-stage half-bridge AC-DC converter with high power factor. *IEEE Transactions on Industrial Electronics*, 48(6), 1219-1225.
- Wang, Y., Guan, Y., Ren, K., Wang, W., & Xu, D. (2015). A single-stage LED driver based on BCM boost circuits and LLC converter for street lighting system. *IEEE Transactions on Industrial Electronics*, 62(9), 5446-5457.
- Wang, Y., Zhang, X., Wang, W., & Xu, D. (2010, Oct 10-13). A novel interleaved single-stage AC/DC converter with high power factor and ZVS characteristic. Paper presented at the International Conference on Electrical Machines and Systems (ICEMS) (pp. 249-254).

